

SCIENTIFIC REPORTS



OPEN

Deletion of the *celA* gene in *Aspergillus nidulans* triggers overexpression of secondary metabolite biosynthetic genes

Gea Guerriero¹ , Lucia Silvestrini², Sylvain Legay¹, Frank Maixner³, Michael Sulyok⁴, Jean-Francois Hausman¹ & Joseph Strauss²

Although much progress has been made in the study of cell wall biosynthetic genes in the model filamentous fungus *Aspergillus nidulans*, there are still targets awaiting characterization. An example is the gene *celA* (ANIA_08444) encoding a putative mixed linkage glucan synthase. To characterize the role of *celA*, we deleted it in *A. nidulans*, analyzed the phenotype of the mycelium and performed RNA-Seq. The strain shows a very strong phenotype, namely “balloons” along the hyphae and aberrant conidiophores, as well as an altered susceptibility to cell wall drugs. These data suggest a potential role of the gene in cell wall-related processes. The Gene Ontology term Enrichment analysis shows increased expression of secondary metabolite biosynthetic genes (sterigmatocystin in particular) in the deleted strain. Our results show that the deletion of *celA* triggers a strong phenotype reminiscent of cell wall-related aberrations and the upregulation of some secondary metabolite gene clusters in *A. nidulans*.

The cell wall is a structure involved in important stages of fungal growth and morphogenesis. Several studies in the literature have shown how perturbations at the cell wall-level trigger dramatic effects on growth¹. Despite the importance of fungal cell walls and despite the great advances made in the field, there are still missing pieces in our understanding of cell wall dynamics in filamentous fungi. Some cell wall biosynthetic genes, for example, are still uncharacterized (a detailed inventory of *Aspergillus nidulans* cell wall-related genes has been previously published²). The chief polysaccharides in the cell wall of the model organism *A. nidulans* are β -glucans (β -1,3-, β -(1,3;1,4)- and β -1,6-glucans), chitin and α -1,3-glucans. No characterization is yet available for the proposed mixed linkage glucan synthase gene *celA* ANIA_08444², while much is known about the chitin and α -1,3-glucan biosynthetic genes in *A. nidulans*^{3–8}. In *A. nidulans* 6 chitin synthase genes have for instance been identified which belong to classes I to VI^{3–7}. *chsC* and *chsA* were proven to play an important role in hyphal wall integrity and conidiophore development⁴, while *chsB* and *chsD* are involved in hyphal growth and conidiation⁵. Interestingly two of the identified chitin synthases possess a myosin-motor head domain⁷, which was shown to be important for the interaction with the cytoskeleton and to play a role for the correct delivery and insertion in the plasma membrane.

Recently, a study on *A. fumigatus* has characterized a protein with significant similarity to ANIA_08444 termed Tft1, an enzyme shown to be responsible for the production of β -(1,3;1,4)-glucans in this organism⁹.

The protein encoded by *celA* is distantly related to plant cellulose synthase-like proteins (CSLs; Fig. 1), it is orthologous to the characterized *A. fumigatus* mixed-linkage glucan synthase Tft1⁹, whose deletion causes no obvious phenotype in *A. fumigatus*, except for a modest increase in virulence.

¹Luxembourg Institute of Science and Technology (LIST), Environmental Research and Innovation (ERIN) Department, Esch/Alzette, L-4362, Luxembourg. ²University of Natural Resources and Life Sciences Vienna (BOKU), Department of Applied Genetics and Cell Biology, Fungal Genetics and Genomics Unit, BOKU Campus, Tulln/Donau, A-3430, Austria. ³European Academy of Bozen/Bolzano (EURAC), Institute for Mummies and the Iceman, Bolzano, 39100, Italy. ⁴University of Natural Resources and Life Sciences Vienna (BOKU), Department for Agrobiotechnology (IFA-Tulln), A-3430, Tulln, Austria. Correspondence and requests for materials should be addressed to G.G. (email: gea.guerriero@list.lu) or J.S. (email: joseph.strauss@boku.ac.at)

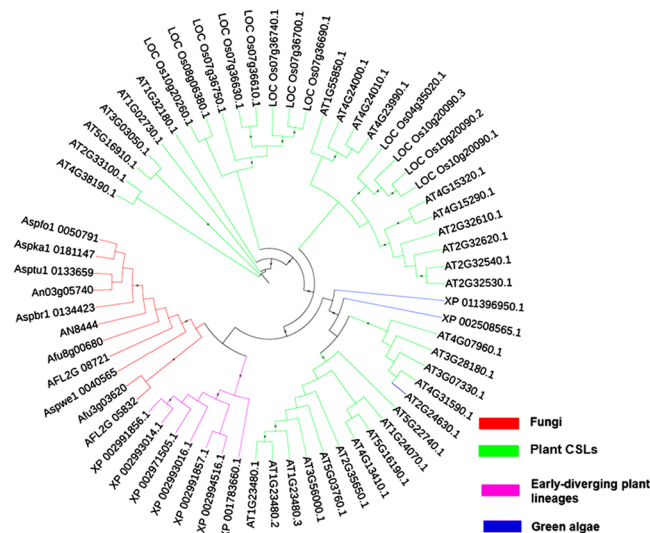


Figure 1. Neighbor-joining tree (bootstraps = 1000) of CelA, its fungal and plant orthologs. Accession numbers are indicated in the tree.

To characterize the role of *celA* in the growth and development of the model filamentous fungus *A. nidulans*, we here sought to provide transcriptomic data of a strain which lacks the gene *celA* (the strain is hereafter referred to as *celA* Δ).

In the present study, we provide experimental evidence for a relationship existing between the deletion of the gene *celA* and the upregulation of genes involved in the production of secondary metabolites (SM). We propose that *celA* partakes in a mechanism regulating SM production in *A. nidulans*.

Results and Discussion

Deletion of *celA* causes a strong phenotype in *A. nidulans*. Transformation of the SAA.111 recipient strain with the replacement cassette containing the *argB* selectable marker yielded three independent transformants; however, subsequent growth cycles of the transformants from conidia on selective medium resulted in one single transformant as capable of stable growth under arginine deprivation. This *celA* Δ strain was analyzed and found to have a single and correct *argB* marker insertion replacing *celA* in the genome (Suppl. Figure 1a; for a schematic representation of the *EcoRI* restriction map in the wild-type and *celA* Δ , see Suppl. Figure 1b). The diagnostic PCRs highlighted the expected shift in MW caused by deletion of *celA* and insertion of the *argB* marker (Suppl. Figure 1c and d).

When grown on solid medium, the *celA* Δ strain showed a macrophenotype: besides growing more slowly, it developed a colony with an outer sector devoid of pigments, as compared to the control (Fig. 2a). The *celA* Δ strain showed decreased sensitivity to the cell wall drugs Congo Red (CR) and dichlobenil (DCB) (Fig. 2b). Microscopic observations of the hyphae in the *celA* Δ strain revealed frequently swollen regions and “balloons”; at higher magnifications these structures appeared vacuolated (Fig. 2c). Additionally, several conidiophores retrieved from plate cultures were aberrant, since they showed bifurcations and hyphae-like metulae (Fig. 2c insets). It is known that *A. nidulans* strains lacking specific chitin synthase genes of class V and VI also show a “balloon” phenotype⁷, which is indicative of a weakened cell wall. The results here obtained therefore suggest a potential implication of *celA* in cell wall-related processes; however its actual role in cell wall biosynthesis awaits experimental validation. As the deletion of genes triggering phenotypes reminiscent of those observed in *celA* Δ is often accompanied by compensatory alterations in expression of genes involved in cell wall biosynthesis¹⁰, we tested some of their representatives. As an example, genes involved in chitin and β -1,3-glucan synthesis (Fig. 3) did not show statistically significant changes, with the exception of *chsA* and the cell wall stress sensor *wscB* which were downregulated in *celA* Δ .

Transcriptome of *celA* Δ . Since a strong phenotype was observed and since the majority of the cell wall biosynthetic genes screened did not show dramatic changes in expression at the RT-qPCR, we decided to perform a transcriptomic analysis to uncover eventual differences in the expression of genes acting in other cellular pathways.

After library preparation, quantification and sequencing, we performed data filtering by setting the \log_2 FC > 1 in absolute value (see Materials and Methods). A total of 1305 genes showed statistically significant changes (Suppl. Information). The Gene Ontology term Enrichment (GOE) analysis carried out using ClueGO (in Cytoscape) with the genes upregulated in *celA* Δ (613 in total, see Suppl. Information) revealed an enrichment of functionally-related genes involved in secondary metabolite biosynthesis, such as members of the sterigmatocystin cluster (*stcL*, *stcW*, *stcV*, *stcU*, *stcS*, *stcK*, *stcJ*, *stcF*, *afIR*, *stcB*, *stcA*), as well as genes involved in yellow-polyketide F9775A/F9775B biosynthesis (*orsA*, *orsB*, *orsC*) and monodictyphenone biosynthesis (*mdpA*, *mdpI*, *mdpH*) (Fig. 4; Suppl. Information). Additionally, two putative SM regulatory genes were also responding to the *celA* Δ deletion by up-regulation (*laeA*, *fhbB*). The results obtained with the GO Term Finder at the

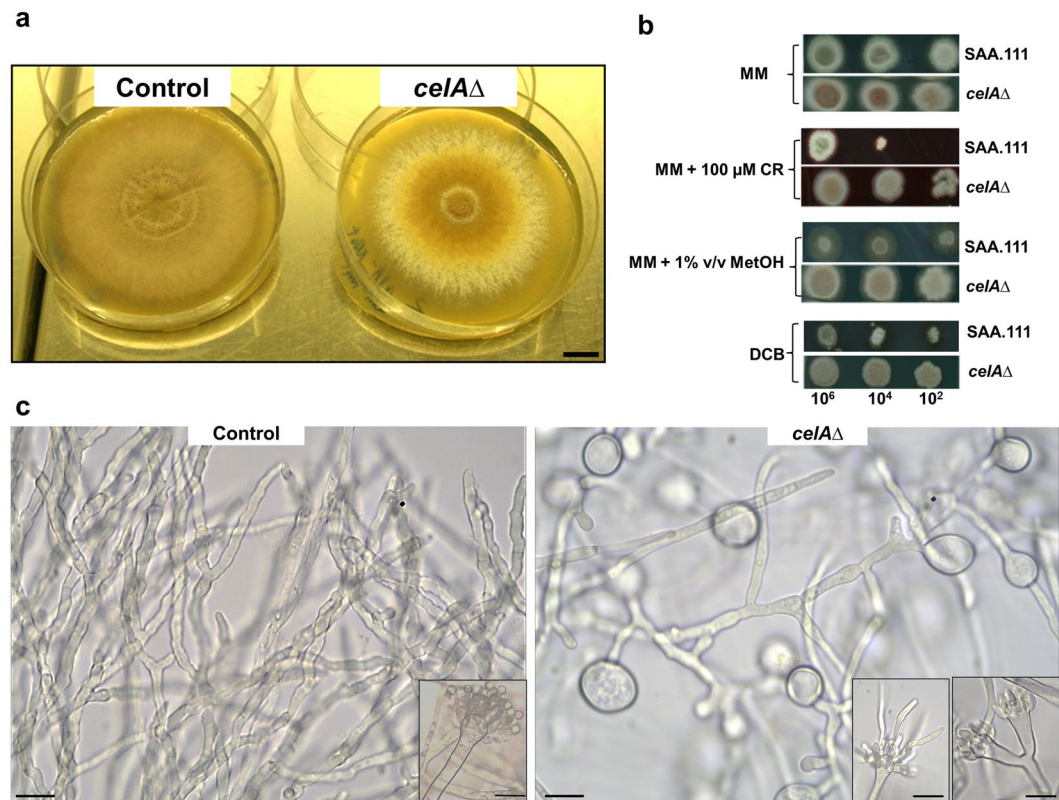


Figure 2. Characterization of the *celAΔ* strain. (a) Macrophenotype of the *celAΔ* strain on solid medium. Bar refers to 1 cm. (b) Sensitivity to the cell wall drugs CR and DCB. Numbers refer to spore dilutions. (c) Balloons along the hyphae and aberrant conidiophores in the *celAΔ* strain. Bars refer to 10 μm.

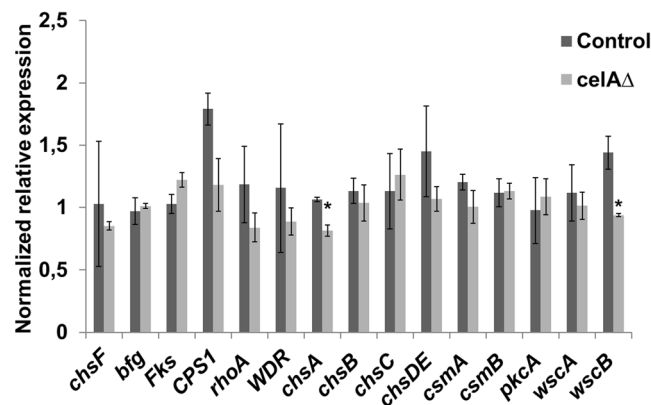


Figure 3. RT-qPCR analysis on a set of cell wall-related genes in the control and *celAΔ* strain. The data were normalized using *rpl3* and *CRP2*. Asterisks indicate statistically significant differences ($p < 0.05$).

AspGD confirmed the enrichment of transcripts involved in secondary metabolic processes in *celAΔ*, with 19 genes involved in toxin biosynthesis (Suppl. Information). The targeted gene expression analysis via RT-qPCR performed on secondary metabolism-related genes (involved in sterigmatocystin, yellow-polyketide F9775A/F9775B and monodictyphenone biosynthesis) confirmed upregulation in *celAΔ* (Fig. 5). Notably, the analysis with the GO Term Finder highlighted a downregulation of genes involved in organonitrogen compound catabolic process: 20 of the identified genes belong to the cellular amino acid catabolic process (Suppl. Information). These data show that, in a manner analogous to what proven in *A. fumigatus*¹¹, an alteration of the cell wall status has an effect on primary metabolism (the primary metabolism is affected with consequent lower abundance of amino acids). Such a phenomenon may be operating in the *celA* mutant, where a stress response is unleashed as a consequence of *celA* deletion and therefore a downregulation of genes belonging to the amino acid biosynthetic process is observed.

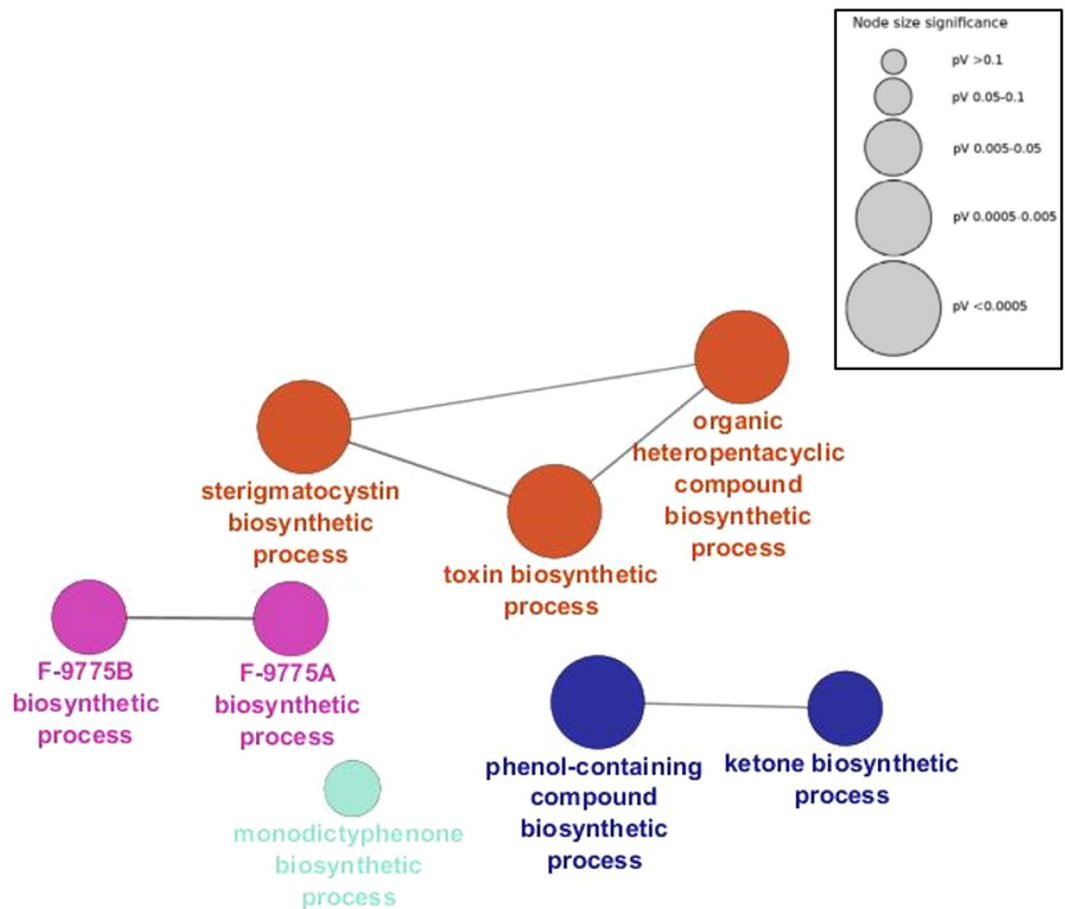


Figure 4. Gene Ontology Enrichment (GOE) analysis of the genes upregulated in *celA*Δ. Gene Ontology (GO) terms sharing similar associated genes are connected with a line. The circle sizes represent different *p*-values (inset).

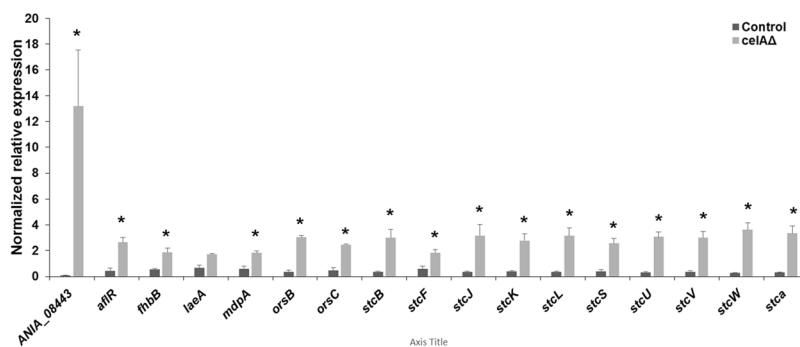


Figure 5. RT-qPCR analysis on ANIA_08443 and a set of secondary metabolism-related genes in the control and *celA*Δ strain. The data were normalized using *rpl3* and *CRP2*. Asterisks indicate statistically significant differences ($p < 0.05$).

High-resolution imaging using scanning electron microscopy (SEM) highlighted a higher number of conidia and conidiophores in *celA*Δ (Fig. 6). In this respect, it should be noted that in the RNA-Seq dataset four conidiation-related genes with increased expression in the mutant are present (Suppl. Information). These genes are: ANIA_05086 ($\log_2FC_{celA\Delta}/ctrl = 3.246$), ANIA_10628 ($\log_2FC_{celA\Delta}/ctrl = 3.236$), ANIA_05015 ($\log_2FC_{celA\Delta}/ctrl = 2.509$), *flbD* ($\log_2FC_{celA\Delta}/ctrl = 1.502$). Interestingly, *flbD* is a member of the fluffy genes required to activate *brlA* and some fluffy mutants are known to display failure to produce sterigmatocystin¹². The higher expression of the Myb transcription factor *flbD* may explain the higher conidiation observed in the mutant, however this is probably not related to the higher sterigmatocystin biosynthesis-related genes, since it was reported that *flbD* overexpression did not trigger an increase in *stc* transcripts¹³. Some secondary metabolites

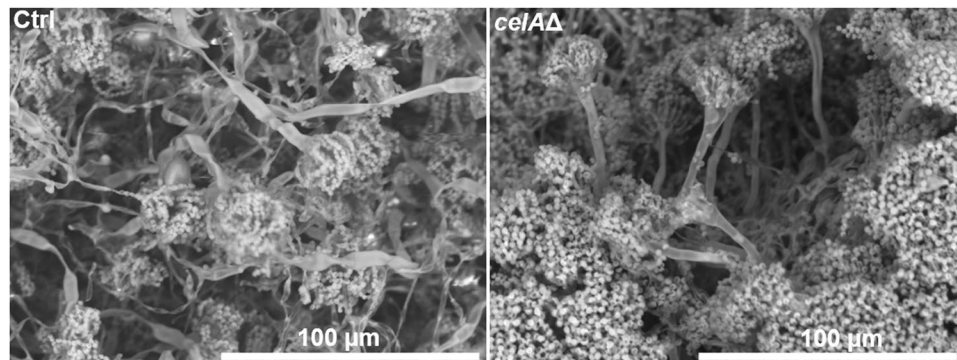


Figure 6. Scanning electron microscope pictures of the control (SAA.111) and *celAΔ*. The deleted strain forms more conidiophores and conidia than the control (the cultures are 4 days old).

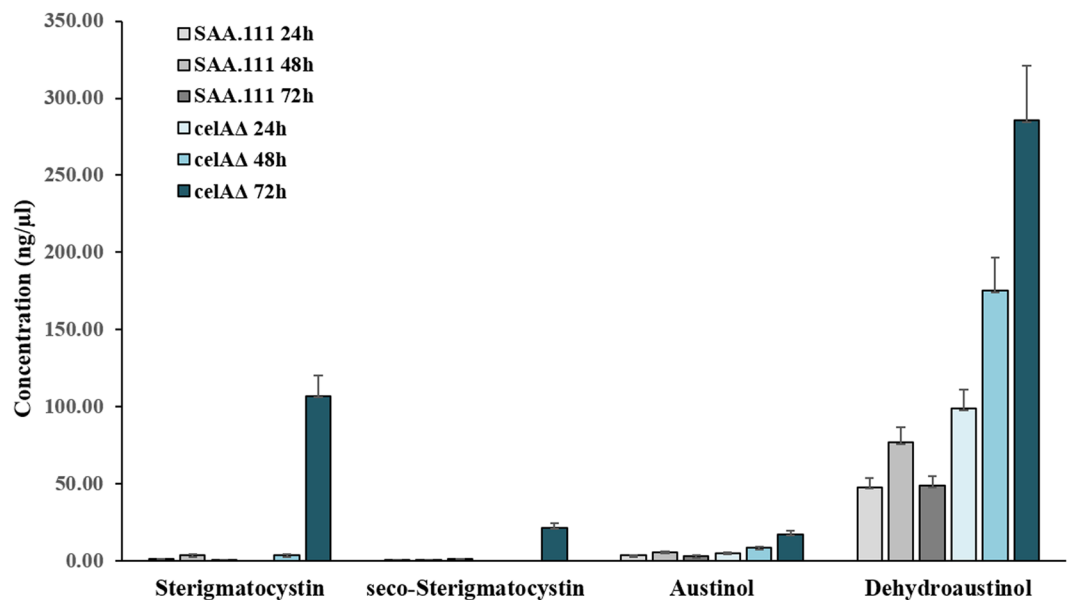


Figure 7. Quantification of some secondary metabolites in the control and *celAΔ* strain.

were quantified using LC-MS/MS at different time-points (24 h–72 h–96 h) and the analysis showed an increase in sterigmatocystin, seco-sterigmatocystin, austinol and dehydroaustinol in *celAΔ* which was the strongest at 96 h (the RNA-Seq time-point) (Fig. 7).

In the light of the observed results, it is here proposed that the increased expression (and production) of secondary metabolites is linked to the sensing of a stress caused or mimicked by the deletion of the gene *celA*.

Under laboratory conditions, many fungal SM gene clusters are cryptic and remain dormant based on a chromatin silencing and inactive signaling pathway¹⁴. They are instead active when the organism is subjected to specific nutritional conditions and/or environmental constraints^{15,16} and enable the colonization of specific natural niches. Manipulations of growth composition can also trigger increased SM biosynthesis, as recently shown with ionic liquids in *A. nidulans*¹⁷. Therefore, the increased expression in SM biosynthetic genes likely reveals a stress status, probably generated by the altered cell wall in *celAΔ*. It should be noted that the deleted strain shows increased resistance to cell wall drugs (Fig. 2b): this is not unexpected, since in the literature it has for instance been shown that, in *A. fumigatus*, deletion of *dvrA*, a transcription factor partaking in cell wall integrity signaling, triggers increased resistance to Nikkomycin Z¹⁸. The phenotypes observed, as well as the altered cell wall drug sensitivity, support the hypothesis of a role of *celA* in a cell wall-related process.

Interestingly, previous studies in the literature on another model fungus, *Hypocrea jecorina*, have shown that a compromised cell wall has consequences on cellulase production: the mutant $\Delta tmk2$ shows increased cellulase production^{19,20}, a feature most likely triggered to favor the growth of a damaged fungal cell, in a manner analogous to what is observed in the $\Delta tmk3$ mutant under solid-state growth¹⁹. Cellulases (as well as other secreted enzymes) may help form a protein layer functioning as an osmotic stabilizer for fungal cells with damaged cell walls¹⁹. It is thus already reported in the literature that alterations in the cell wall influence complex cellular processes, namely the production and secretion of cellulases.

In our dataset, the second gene showing the highest expression in *celA*Δ with respect to the isogenic wild type is ANIA_08443, a gene with no known function. This gene shows a log₂ FC increase in expression of 8.74 (which means it is expressed ca. 429 times more in *celA*Δ than the control). The targeted RT-qPCR analysis confirms upregulation of ANIA_08443 in *celA*Δ (Fig. 5). It should be noted that this gene is adjacent to the *celA* locus and up-regulation could be a coincidental consequence of marker gene insertion at the place of the *celA* gene. However, the BLASTP analysis indicates that the corresponding protein has a DUF3431 domain and predicted to possess a transmembrane region (prediction made with TMHMM v2.0 <http://www.cbs.dtu.dk/services/TMHMM/> and Phobius <http://phobius.sbc.su.se/>) and to expose a large portion including the C-terminus to the cell's exterior (Suppl. Information; residues 27–384 according to TMHMM and 37–384 according to Phobius). Therefore, we cannot exclude that this protein may represent a sensor of the cell wall status. More specifically, this uncharacterized protein may represent a potential candidate involved in cell wall status sensing and signal transduction to the cell's interior. Its role in signal transduction and activation of SM biosynthetic gene clusters awaits validation via functional studies, nevertheless the results shown pave the way to future studies on *celA*, as well as on the link between cell wall alterations and SM production in *A. nidulans*. In this respect we believe important to mention that a DUF3431 protein was shown to be upregulated upon salt stress in the halotolerant fungus *A. glaucus*²¹ and to confer increased stress tolerance when expressed heterologously in *Arabidopsis* plants.

Future functional studies should provide evidence for an implication of this gene in cell wall status sensing and SM production in *A. nidulans*.

Materials and Methods

Deletion of *celA* in *A. nidulans*. The strain used in this study is SAA.111 (genotype *veA1; biA1; ΔargB::trpC; riboB2; pyroA4; wA3*)²². Gene replacement of ANIA_08444 was performed with the double joint-PCR (DJ-PCR)²³: the cassette containing the selectable marker *argB* (ANIA_04409) was inserted to replace the entire locus ANIA_08444. The *argB* gene was amplified from plasmid pMS12²⁴. Transformation was carried out as described previously²².

The primers used for the DJ-PCR are indicated in Suppl. Information.

PCRs to create the replacement cassette were performed with the Phusion High-Fidelity PCR Master Mix, according to the manufacturer's instructions. Optimal annealing temperatures were computed with the NEB Tm calculator v1.9.4 (<http://tmcalculator.neb.com/#!/>).

Deletion was checked via Southern blotting, which provided clear evidence of deletion (Suppl. Figure 1a), however RNA-Seq, due to its high sensitivity, detected very low background expression levels of *celA* (average 3.8 RPKM). This expression level was however negligible and probably due to contaminating residual heterokaryons; it was not relevant to the further characterization of *celA*Δ, whose phenotype is reminiscent of already characterized cell wall mutants⁷. Southern blotting (DNA cut with *EcoRI* and DIG-labelled probe amplified with primers *celA* Upstream Fwd and *celA* Downstream Rev), diagnostic PCR on genomic DNA (gDNA) and RT-qPCR were performed as described previously²⁵. Diagnostic PCRs using gDNA were performed with the Q5 Hot-Start High-Fidelity Master Mix, using the primers *celA* nested Fwd and *celA* nested Rev (Suppl. Information); the annealing temperature was set at 64 °C with an extension of 3 minutes and a total of 30 amplification cycles on a Veriti Thermal Cycler. The primers of the reference genes *rpl37*, *rpl3*, *CRP2* and actin used for the RT-qPCR have been previously reported²⁴. The RT-qPCR primers used to amplify the additional reference gene *H2B*, as well as those relative to the secondary metabolism genes are in Suppl. Information. Optical microscopy and growth test in the presence of cell wall drugs were performed as previously described²⁶.

RT-qPCR, RNA-Seq and bioinformatics. Libraries were prepared from 3 μg of total RNA extracted from the mycelium after 3 days of growth at 37 °C with the SMARTer Stranded RNA-Seq kit (Clontech). The isolation of mRNAs was performed using the Illumina beads and the TruSeq protocol (Illumina), as previously described²⁷. The synthesis of cDNA and shearing were performed with ten ng of mRNA, according to the manufacturer's instruction. The enrichment step was carried out using 14 cycles of PCR. The libraries were then checked using a 2100 Bioanalyzer (DNA High sensitivity Kit) to estimate the average fragment size. Library quantification was performed using the KAPA library quantification kit (KAPA Biosystems) and a ViiA7 Real-Time PCR System (Life technologies). The pooled libraries (at a concentration of 20 pM) were sequenced on an Illumina MiSeq (MiSeq reagent kit V3, 150 cycles) generating 76 base pairs paired-end reads. Raw sequences have been deposited at the NCBI Gene Expression Omnibus (GEO), <http://www.ncbi.nlm.nih.gov/geo/>, under the accession number GSE94110 (link to access the data <https://www.ncbi.nlm.nih.gov/geo/query/acc.cgi?token=qnojukmnmnzifxq&acc=GSE94110>).

Raw FASTA files were imported in CLC Genomics Workbench 9.0.1. Sequences were filtered and trimmed according to the following criteria: sequence length > 35 base pairs (bp), sequence quality score < 0.01, no ambiguity in the sequence, trimming using Illumina adaptors, hard trim of 8 bp at the 5' end and 2 bp at the 3' end, resulting in a longest length of 64 bp. For each library, the mapping against the *A. nidulans* FGSC A4 transcriptome (downloaded at the http://www.aspergillusgenome.org/download/sequence/A_nidulans_FGSC_A4/current/) was performed with the following settings: a maximum hit per reads of 3, similarity fraction = 0.9, a length fraction = 0.9, a mismatch, insertion and deletion cost of 3 (stringent mapping). The expression values were then calculated using the RPKM method²⁸. In order to highlight the differentially expressed genes, a t-test with 2 groups (control and *celA*Δ, each composed of three biological replicates) was performed. Only genes with a *p*-value below 0.05 were selected. A cut-off threshold was also applied to the fold change (log₂ FC absolute value > 1).

The GOE analysis was carried out using loci with log₂ FC > 1 (i.e. overexpressed in *celA*Δ) using ClueGO (v2.3.2)²⁹ within Cytoscape (v3.4.1) with the following parameters: gene ontology from level 3 to level 8, kappa

score set at 0.6, p -value < 0.05, enrichment analysis with a Benjamini–Hochberg correction. The GO analysis was also carried out using the GO Term Finder at the AspGD (<http://www.aspergillusgenome.org/cgi-bin/GO/goTermFinder>).

Full-length protein sequences (accessions indicated in the tree) were aligned with ClustalOmega (<http://www.ebi.ac.uk/Tools/msa/clustalo>) and the alignment was submitted to PHYML (<http://www.phylogeny.fr>). The tree was visualized with iTOL-Interactive Tree Of Life (<http://itol.embl.de/>).

SEM and metabolite profiling by LC-MS/MS. The analysis at the SEM was carried out as previously described²⁶. LC-MS/MS screening of target fungal metabolites was performed with a QTrap 5500 LC-MS/MS System (Applied Biosystems, Foster City, CA) equipped with a TurboIonSpray electrospray ionization (ESI) source and an 1290 Series HPLC System (Agilent, Waldbronn, Germany). Chromatographic separation was performed at 25 °C on a Gemini[®] C18-column, 150 × 4.6 mm i.d., 5 μm particle size, equipped with a C18 4 × 3 mm i.d. security guard cartridge (all from Phenomenex, Torrance, CA, US). The chromatographic method, as well as the chromatographic and mass spectrometric parameters, have been previously described³⁰, but the method has in the meantime been expanded to cover 650 metabolites (manuscript in preparation).

References

- Horiuchi, H. Functional diversity of chitin synthases of *Aspergillus nidulans* in hyphal growth, conidiophore development and septum formation. *Med. Mycol.* **47**(Suppl 1), S47–52 (2009).
- de Groot, P. W. J. *et al.* Comprehensive genomic analysis of cell wall genes in *Aspergillus nidulans*. *Fungal Genet. Biol. FG B* **46**(Suppl 1), S72–81 (2009).
- Horiuchi, H., Fujiwara, M., Yamashita, S., Ohta, A. & Takagi, M. Proliferation of intrahyphal hyphae caused by disruption of *csmA*, which encodes a class V chitin synthase with a myosin motor-like domain in *Aspergillus nidulans*. *J. Bacteriol.* **181**, 3721–3729 (1999).
- Fujiwara, M. *et al.* Evidence that the *Aspergillus nidulans* class I and class II chitin synthase genes, *chsC* and *chsA*, share critical roles in hyphal wall integrity and conidiophore development. *J. Biochem. (Tokyo)* **127**, 359–366 (2000).
- Ichinomiya, M. *et al.* Repression of *chsB* expression reveals the functional importance of class IV chitin synthase gene *chsD* in hyphal growth and conidiation of *Aspergillus nidulans*. *Microbiology* **148**, 1335–1347 (2002).
- Ichinomiya, M., Yamada, E., Yamashita, S., Ohta, A. & Horiuchi, H. Class I and Class II Chitin Synthases Are Involved in Septum Formation in the Filamentous Fungus *Aspergillus nidulans*. *Eukaryot. Cell* **4**, 1125–1136 (2005).
- Takeshita, N., Yamashita, S., Ohta, A. & Horiuchi, H. *Aspergillus nidulans* class V and VI chitin synthases *CsmA* and *CsmB*, each with a myosin motor-like domain, perform compensatory functions that are essential for hyphal tip growth. *Mol. Microbiol.* **59**, 1380–1394 (2006).
- Yoshimi, A. *et al.* Functional Analysis of the α-1,3-Glucan Synthase Genes *agsA* and *agsB* in *Aspergillus nidulans*: *AgbB* Is the Major α-1,3-Glucan Synthase in This Fungus. *PLoS ONE* **8**, e54893 (2013).
- Samar, D., Kieler, J. B. & Klutts, J. S. Identification and deletion of *Tft1*, a predicted glycosyltransferase necessary for cell wall β-1,3,1,4-glucan synthesis in *Aspergillus fumigatus*. *PLoS One* **10**, e0117336 (2015).
- García-Rodríguez, L. J. *et al.* Characterization of the chitin biosynthesis process as a compensatory mechanism in the *fks1* mutant of *Saccharomyces cerevisiae*. *FEBS Lett* **478**, 84–88 (2000).
- Jain, R. *et al.* The MAP kinase MpkA controls cell wall integrity, oxidative stress response, gliotoxin production and iron adaptation in *Aspergillus fumigatus*. *Mol. Microbiol.* **82**, 39–53 (2011).
- Wieser, J., Yu, J. H. & Adams, T. H. Dominant mutations affecting both sporulation and sterigmatocystin biosynthesis in *Aspergillus nidulans*. *Curr. Genet.* **32**, 218–224 (1997).
- Hicks, J. K., Yu, J.-H., Keller, N. P. & Adams, T. H. *Aspergillus* sporulation and mycotoxin production both require inactivation of the Fada Gα protein-dependent signaling pathway. *EMBO J* **16**, 4916–4923 (1997).
- Gacek, A. & Strauss, J. The chromatin code of fungal secondary metabolite gene clusters. *Appl. Microbiol. Biotechnol.* **95**, 1389–1404 (2012).
- Lim, F. Y., Sanchez, J. F., Wang, C. C. C. & Keller, N. P. Toward Awakening Cryptic Secondary Metabolite Gene Clusters in Filamentous Fungi. *Methods Enzymol* **517**, 303–324 (2012).
- Brakhage, A. A. Regulation of fungal secondary metabolism. *Nat. Rev. Microbiol.* **11**, 21–32 (2013).
- Alves, P. C. *et al.* Transcriptomic and metabolomic profiling of ionic liquid stimuli unveils enhanced secondary metabolism in *Aspergillus nidulans*. *BMC Genomics* **17**, 284 (2016).
- Ejzykiewicz, D. E. *et al.* Role of *Aspergillus fumigatus* DvrA in host cell interactions and virulence. *Eukaryot. Cell* **9**, 1432–1440 (2010).
- Wang, M. *et al.* A Mitogen-Activated Protein Kinase Tmk3 Participates in High Osmolarity Resistance, Cell Wall Integrity Maintenance and Cellulase Production Regulation in *Trichoderma reesei*. *PLoS One* **8**, e72189 (2013).
- Wang, M. *et al.* Identification of the role of a MAP kinase Tmk2 in *Hypocrea jecorina* (*Trichoderma reesei*). *Sci. Reports* **5**, 11875 (2014).
- Fang, J. *et al.* Isolation of Salt Stress-Related Genes from *Aspergillus glaucus* CCHA by Random Overexpression in *Escherichia coli*. *Sci. World J.* **2014** (2014).
- Bernreiter, A. *et al.* Nuclear Export of the Transcription Factor NirA Is a Regulatory Checkpoint for Nitrate Induction in *Aspergillus nidulans*. *Mol. Cell. Biol.* **27**, 791–802 (2007).
- Yu, J.-H. *et al.* Double-joint PCR: a PCR-based molecular tool for gene manipulations in filamentous fungi. *Fungal Genet. Biol.* **41**, 973–981 (2004).
- Schinko, T., Gallmetzer, A., Amillis, S. & Strauss, J. Pseudo-constitutivity of nitrate-responsive genes in nitrate reductase mutants. *Fungal Genet. Biol.* **54**, 34–41 (2013).
- Guerriero, G. *et al.* A WDR Gene Is a Conserved Member of a Chitin Synthase Gene Cluster and Influences the Cell Wall in *Aspergillus nidulans*. *Int. J. Mol. Sci.* **17**, 1031 (2016).
- Guerriero, G. *et al.* Sensitivity of *Aspergillus nidulans* to the cellulose synthase inhibitor dichlobenil: insights from wall-related genes' expression and ultrastructural hyphal morphologies. *PLoS One* **8**, e80038 (2013).
- Behr, M. *et al.* Studying Secondary Growth and Bast Fiber Development: The Hemp Hypocotyl Peeks behind the Wall. *Front. Plant Sci.* **7**, 1733 (2016).
- Mortazavi, A., Williams, B. A., McCue, K., Schaeffer, L. & Wold, B. Mapping and quantifying mammalian transcriptomes by RNA-Seq. *Nat. Methods* **5**, 621–628 (2008).

29. Bindea, G. *et al.* ClueGO: a Cytoscape plug-in to decipher functionally grouped gene ontology and pathway annotation networks. *Bioinforma. Oxf. Engl* **25**, 1091–1093 (2009).
30. Malachová, A., Sulyok, M., Beltrán, E., Berthiller, F. & Krska, R. Optimization and validation of a quantitative liquid chromatography-tandem mass spectrometric method covering 295 bacterial and fungal metabolites including all regulated mycotoxins in four model food matrices. *J. Chromatogr. A* **1362**, 145–156 (2014).

Acknowledgements

GG gratefully acknowledges the support by the Austrian Science Fund (FWF; <http://www.fwf.ac.at/en/>) Grant No. M1315. Work in the lab of JS was supported by the “EpiMed” NFB grant LS12–009.

Author Contributions

G.G. conceived the idea of writing the paper. G.G. constructed the *celA*Δ strain, analyzed the phenotype at the optical microscope, performed the Southern blotting, diagnostic PCRs, RT-qPCR, RNA-Seq and bioinformatics. L.S. grew the strains in liquid culture, performed the Southern blotting and contributed to the microscopic analysis. S.L. and F.M. contributed to the bioinformatics. M.S. performed secondary metabolite quantification. G.G., L.S., S.L., F.M., M.S., J.F.H. and J.S. interpreted the data and wrote the manuscript.

Additional Information

Supplementary information accompanies this paper at doi:[10.1038/s41598-017-05920-x](https://doi.org/10.1038/s41598-017-05920-x)

Competing Interests: The authors declare that they have no competing interests.

Accession codes: Raw reads were deposited at the NCBI Gene Expression Omnibus (GEO), under accession GSE94110.

Publisher's note: Springer Nature remains neutral with regard to jurisdictional claims in published maps and institutional affiliations.



Open Access This article is licensed under a Creative Commons Attribution 4.0 International License, which permits use, sharing, adaptation, distribution and reproduction in any medium or format, as long as you give appropriate credit to the original author(s) and the source, provide a link to the Creative Commons license, and indicate if changes were made. The images or other third party material in this article are included in the article's Creative Commons license, unless indicated otherwise in a credit line to the material. If material is not included in the article's Creative Commons license and your intended use is not permitted by statutory regulation or exceeds the permitted use, you will need to obtain permission directly from the copyright holder. To view a copy of this license, visit <http://creativecommons.org/licenses/by/4.0/>.

© The Author(s) 2017